Investigation of Sensor Parameters for Kinematic Assessment of Steady State Running Using Foot Mounted IMUs

G. P. Bailey and R. K. Harle
Computer Laboratory, University of Cambridge, William Gates Building, 15 JJ Thomson Avenue, Cambridge, U.K.

Keywords: Running, Gait, Foot Kinematics, Continuous Sensing, Sampling Rates, Sensor Requirements, Impact Acceleration.

Abstract: The continuous sensing of kinematics provides an opportunity to monitor changes in sporting technique or to aid in injury rehabilitation. Inertial sensors are now small enough to integrate into footwear, providing a potential platform for continuous monitoring that does not require additional components to be worn by the athlete and can be used to assess foot kinematics during running. To facilitate widespread adoption, sensor systems must be as cheap as possible. To achieve this it is required that such systems be engineered with sampling rates that are not unnecessarily high and with sensor components that meet the requirements of the task, including required accuracy. We investigate multiple sensor parameters (sampling rate, acceleration range) and their effect on the accuracy of kinematic assessment using foot worn inertial sensors. We find that Extended Kalman Filter based trajectory recovery seems to be little affected by sampling rates until below 250Hz. We investigate impact accelerations using an inertial measurement unit attached to the foot and find that, at 250Hz, the acceleration signal peaks at up to 70g around heel strike.

1 INTRODUCTION

Biomechanical assessment of movement is a complicated but valuable component of today's elite sports training. Assessment of running gait is particularly important and is usually performed within a laboratory setting using video or optical motion capture. These assessments are often characterised by expensive equipment, manual analysis and subjective metrics. Furthermore the restricted space of a laboratory necessitates evaluation either using a small number of steps or, more often, a treadmill. In neither case is the athlete free to move naturally and there is little guarantee that the gait exhibited is that found in the true sporting arena.

In order to address these issues and to bring such kinematic assessment to a wider audience, low-cost inertial sensors are being embedded within consumer products, allowing athletes to be assessed in their natural setting and, additionally, more frequently. Such in-field constant-assessment brings with it additional benefits, including tracking the progress of injury rehabilitation and enabling longitudinal sports science and biomechanical studies.

Foot-mounted sensors are popular since lightweight sensors can be embedded within shoes in a convenient, unobtrusive way. They may be able to capture rich data, and have already attracted commercial interest (e.g. the Nike+ shoe). In the future, such sensors may be able to track relevant performance metrics or detect compensatory patterns that are the result of poor biomechanics.

Previous studies have shown that foot-worn sensors are capable of providing a full three dimensional trajectory of the foot during steady state running (Bailey and Harle, 2014) and walking (Mariani et al., 2010) when combined with the inertial strapdown navigation algorithm. This allows various metrics to be calculated that may be of use to coaches or biomechanists, for example peak foot height or mean step velocity. Our previous work found that that usable results could be achieved using both an Extended Kalman Filter and a linear dedrifting technique in combination with the strapdown algorithm (Bailey and Harle, 2014). The work also suggested limitations in the accelerometer resulted in short periods of sensor saturation around heel strike, and that this may have compromised results.

The purpose of this study is to assess the effect of sensor parameters on the accuracy of tracking the three dimensional trajectory of the foot during steady state running.

P. Bailey G. and K. Harle R..
Investigation of Sensor Parameters for Kinematic Assessment of Steady State Running Using Foot Mounted IMUs.
DOI: 10.5220/0005093601540161
In *Proceedings of the 2nd International Congress on Sports Sciences Research and Technology Support* (icSPORTS-2014), pages 154-161
ISBN: 978-989-758-057-4

We address the following research questions:

- *How do sampling rates affect the accuracy of trajectory recovery?*
  Below a certain point, lower sampling rates might be expected to produce less accurate results. At what point does the sampling rate compromise results? There will be a trade off with sensor requirements.
- *What are the requirements of inertial sensors in terms of range?*
  In order to capture the trajectory of the foot using inertial sensors, the captured signals should not contain periods of saturation. The required range of the sensor will depend on the sampling rate used. For lower sampling rates, higher frequencies will be attenuated during the low pass filter stage reducing requirements on the sensor. The running surface may also affect the sensor requirements and so we include outdoor running on a variety of surfaces.
- *How much does a small amount of sensor saturation affect results?*
  Our previous study found that any sensor saturation usually happens at heel strike and typically only for a few milliseconds (Bailey and Harle, 2014). Is it necessary to have a high range inertial sensor or do periods of sensor saturation have minimal affect on the accuracy of the results?

In answering these questions we will structure the paper as follows. A section detailing the experimental platform will be provided, followed by a section for each of the research questions outlined above. These sections will contain methods and results for the experiment required to answer each question. We will conclude by discussing how the results of each of the three experiments trade off.

2 BACKGROUND

Limited research has been conducted with foot worn sensors for running. However, some studies have looked at impact accelerations at heel strike with sensors attached to the shank. For example, (Mizrahi, 2000) investigated the effect of fatigue on impact accelerations by attaching a $\pm 50g$ accelerometer to the tibial tuberosity. A high sampling rate was used (1667Hz) and the authors found during the study that the average impact acceleration increased with fatigue to $11.1 \pm 4.2g$. However, impact accelerations at the tibial tuberosity are likely to be much smaller than those present at the foot.

Strapdown techniques have previously been investigated for use in assessing running kinematics but sensor saturation was found around heel strike using a $\pm 16g$ sensor at 1kHz (Bailey and Harle, 2014). Another study (Bichler et al., 2012) used a similar technique with a 100Hz sampling rate but limitations in the video reference system used as ground truth make it difficult to compare the two studies in terms of accuracy.

For pedestrian localisation applications, optimal sampling frequency has been investigated (Munoz Diaz et al., 2013). Although the authors did investigate a wide range of scenarios including running, they did not evaluate the effects lower sampling rates had on accuracy for running. They concluded from a frequency based analysis that the lowest usable sampling rate for running would be 300Hz.

3 SENSOR PLATFORM AND DATA CAPTURE

The sensor platform and methods common to each part of the paper will be described in the following section.

3.1 Inertial Sensors

Capture of inertial sensor data was facilitated using the ION (Imperceptible On-body Node) sensor platform (Harle et al., 2011) with the addition of an Inertial Measurement Unit (IMU) providing a three-axis $\pm 16g$ accelerometer and $\pm 2000^{\circ}s^{-1}$ gyroscope (MPU-6000, InvenSense Inc.) and containing an internal 16 bit Analog-Digital Converter (ADC).

Additionally an analogue three-axis accelerometer (ADXL377, Analog Devices Inc.) with a $\pm 200g$ range was included on the same PCB as the MPU-6000, mounted on the reverse side such that both sensors were co-located to expose them to the same motion. The ADXL377 was connected to the ION sensor platform's 14 bit ADC.

The sensor platform is lightweight, weighting approximately 15 grams in total, including battery.

The platform was extended to contain two accelerometers due to sensor saturation observed in earlier experiments. The lower $16g$ range sensor was used to capture the majority of the data with the $200g$ sensor capturing the high frequency peaks that occur near heel strike.

The MPU-6000 has an internal Digital Low Pass Filter, meaning the accelerometer and gyroscope signals on the MPU-6000 had a bandwidth of 260Hz and

256Hz respectively. The analogue accelerometer was set up with a 500Hz bandwidth.

All IMU signals were sampled at 1kHz and logged to on-board flash memory. In all experiments the ION sensor was placed on the lateral side of the shoe in line with the ankle, as seen in Figure 1. The sensor was firmly taped to the outside of the shoe to simulate the scenario where it was built into the shoe, perhaps embedded in the sole in a similar manner to the Nike+ shoe. Finally the validity of the zero-velocity assumption (Foxlin, 2005) used in foot mounted inertial navigation techniques has been evaluated (Peruzzi et al., 2011). The study investigates different mounting locations on the foot and shows that the sensor position we have used is among the best suited to using this assumption.

3.2 Ground Truth

Ground truth, where applicable, was captured using an optical motion capture system (Vicon Motion Systems, UK) sampling at 240Hz.

For experiments requiring ground truth, a treadmill was used in order to capture many steps in a limited motion capture area. While the biomechanics of treadmill running may be different to overground running, results should be applicable to kinematic assessment of overground running. This follows from the observation that, from a sensing perspective, treadmill running differs from overground running only in frame of reference.

The treadmill was set up without any inclination as measured with a spirit level. The ION sensor was attached to a custom jig containing 3 retro-reflective markers (Fig. 1) for the motion capture system. The jig adds an additional 30 grams of weight to the system (45 grams total, including ION) but remains comfortable for test runs. The jig was laser cut and the MPU-6000 and retro-reflective markers were aligned with laser-etched outlines to ensure alignment between the jig and the inertial sensor axes.

Figure 1: Shoe with IMU and Jig for facilitating ground truth capture using the Vicon Motion capture system.

3.3 Combining Accelerometer Signals

Our previous work shows that for treadmill running at 3.4m/s and below, and at a sampling rate of 1kHz, sensor saturation is present in the accelerometer signals when a 16g accelerometer is in use for short periods of time (Bailey and Harle, 2014).

Since the majority of the step contains signals within the 16g range and only a few samples per step are saturated, the 16g accelerometer data was used. Any sensor saturation was corrected for using the 200g accelerometer to 'fill-in' the saturated samples. This means that the lower noise and higher resolution (16 bit vs. 14 bit) of the MPU-6000 (16g) was utilised for the majority of the step.

Combination of the accelerometer signals was done in the following way. In order to avoid any artifacts produced by sensor nonlinearities near the limit of the MPU-6000s range, samples with a value greater than 140ms^{-2} were replaced by those from the higher range sensor. When applicable, this replacement was done before any further processing (e.g. down-sampling).

4 METHODS AND RESULTS

In order to address the research questions outlined in section 1, a number of experiments were designed to test sensor requirements. The methods and results of each experiment are described in this section.

4.1 Effect of Sampling Rates

In order to assess sensor requirements at varying sampling rates, inertial data were collected at a 1kHz sampling rate before being digitally downsampled to simulate lower sampling rates.

Four participants took part in the study (2 male, 2 female). All participants had a heel-strike running pattern. Ethics committee approval was obtained. Participants were asked to warm up on the treadmill for a few minutes to familiarise themselves with the environment and treadmill speeds. Once the warm up period was complete, the athlete rested for two minutes as the experimental process was explained. Four ninety-second runs were completed, with data logging, by each participant. Data logging included inertial data and motion capture data as described previously. Each run was performed at a predetermined treadmill speed, approximately 2.3ms^{-1}, 2.7ms^{-1}, 3.0ms^{-1} and 3.4ms^{-1}, as measured by the Vicon system. Prior to and immediately after each run, the athlete was asked to stamp their feet three times in order to facilitate simple synchronisation between the Vicon and ION systems. A single sensor placed on the right foot was used to conduct the experiment. Due

to the acceleration and deceleration of the treadmill at the start and end of each run the middle 90 steps were taken from each run to provide a total of 1440 steps for analysis.

Once data collection was complete the signals were subsequently downsampled in order to simulate lower sampling rates. Integer downsampling factors were used so that interpolation was avoided.

Downsampling for a given downsampling factor, M, proceeded as a two step process. Firstly, to avoid aliasing affects, the data was low-pass filtered. A 4th order butterworth filter was used with a cut off frequency of $0.8fs_t$ where $fs_t = \frac{fs_b}{M}$ and fs_t is the target sampling rate with fs_b the base sampling rate used by the ION sensor platform (always 1kHz). Secondly, the resulting signal was decimated by retaining every M^{th} sample.

An Extended Kalman Filter (EKF), paired with an inertial strapdown algorithm, was used to recreate the trajectory of the foot from the inertial data (Bailey and Harle, 2014; Foxlin, 2005). The speed of the treadmill belt was applied as a pseudo measurement during the mid-stance phase of gait along with a zero-foot height pseudo measurement.

As an example of the kind of output that this technique can enable, Figure 2 contains two example steps from two different people running at the same speed. Differences in technique can be seen between the two in these 2D plots. While 3D plots are possible we use a 2D plot here to make the differences clearer.

This method was applied to each run from each participant at each downsampling factor. The downsampling factors used produced the equivalent of 500Hz, 250Hz, 125Hz, and 62.5Hz in addition to the 1000Hz raw signal.

The technique creates a rich set of data detailing the velocity, position and angle of the foot at the time each inertial sample was taken. For trajectory evaluation the position, velocity and attitude error is calculated for each step. Errors are calculated stepwise as offsets in position at the start of the step are irrelevant for an assessment of the step, therefore the ground truth and inertial solutions are aligned in space before calculating the following metrics.

Position error was calculated in the following way:

$$s^{error}(i,k) = \|\mathbf{s}^{inertial}(i,k) - \mathbf{s}^{vicon}(i,k)\| \quad (1)$$

and velocity error was calculated as:

$$v^{error}(i,k) = \|\mathbf{v}^{inertial}(i,k) - \mathbf{v}^{vicon}(i,k)\| \quad (2)$$

where i is the step number and k sample number within step i. Error in attitude was assessed as

$$\theta^{err}(i,k) = \arccos\left(\frac{\mathbf{A}.\mathbf{B}}{\|\mathbf{A}\|\|\mathbf{B}\|}\right) \quad (3)$$

Where $\mathbf{A}$ and $\mathbf{B}$ represent the vector $[0,0,1]^T$ in the sensor's frame of reference as measured by the INS solution and Vicon respectively.

Figure 3 shows how sampling rates affect the mean error in position, velocity and attitude. The graphs show that with sampling rates lower than 250Hz the position and velocity error starts to increase rapidly meaning that 1kHz is unnecessary and in order to reduce sensor requirements a lower sampling rate may be used without a large affect on accuracy up to 250Hz. Attitude errors were not as affected by lower sampling rates staying stable until 125Hz.

Examples of the full 3D trajectory recovered by the system are shown for two representative steps in Figure 4 where the lower sampling rate has resulted in much poorer performance.

4.2 Sensor Requirements

In order to find optimal sensor parameters we conducted an experiment to determine the requirements for the range of the accelerometer and gyroscope. This is important to make sure that sensors do not saturate during running as this may impair the accuracy of the measurement obtained using strapdown techniques.

Parameters that affect these requirements are sampling rate, running speed and the characteristics of the running surface.

Sampling rates affect sensor requirements due to the low pass filtering required before the signals enter the ADC. Before sensor signals are quantised, it is usually necessary to low-pass filter the signal (in the analogue domain) to a bandwidth of less than half of the sampling rate (Nyquist rate) to ensure aliasing artifacts are avoided. This low-pass filtering has the effect of reducing peak accelerometer and gyroscope signals. Sensor range requirements are therefore reduced as the sampling rate is also reduced. We therefore assess peak accelerations for running while using differing sampling rates.

The accuracy of the algorithms used in (Bailey and Harle, 2014) to assess running kinematics have, so far, been assessed using a treadmill. While in use treadmills may flex visibly as the runner hits the treadmill belt. This may reduce the peak accelerations observed at impact. Since the primary use case of such sensing is in overground running outside, we investigated the effect of a number of outdoor surfaces on the sensor range requirements as these are likely to be larger than for a treadmill. For example, impact accelerations on tarmac are likely to be distinct from those of grass or treadmill running.

Accelerometer and gyroscope data were collected

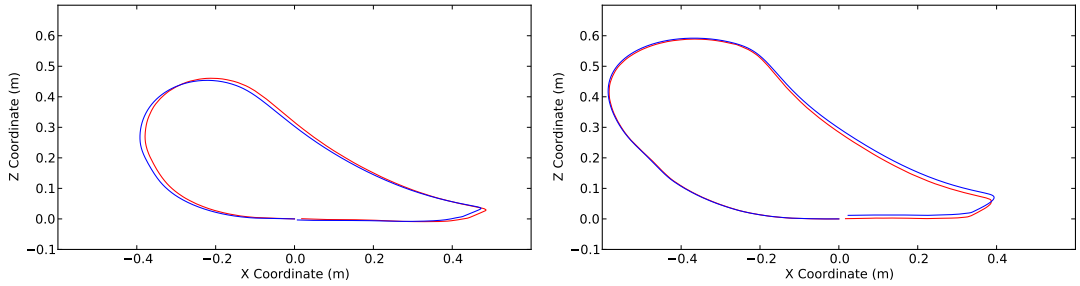

(a) Participant A (b) Participant B

Figure 2: 2D plots of position taken from inertial sensor data and ground truth using a motion capture system. The red line represents ground truth and the blue the inertial solution. Both solutions taken from running on a treadmill at 3.4ms^{-1}.

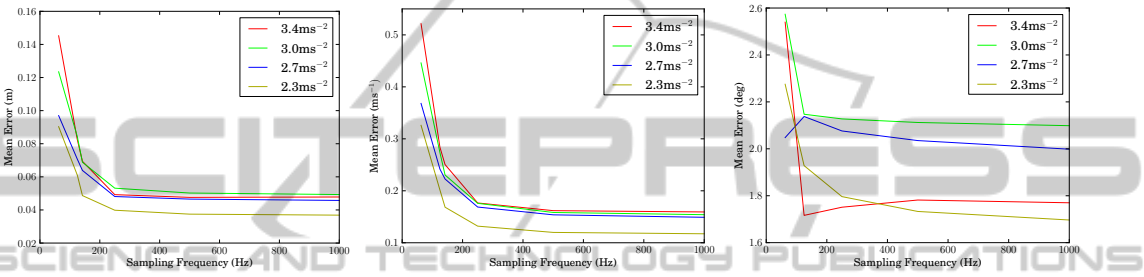

(a) Position (b) Velocity (c) Attitude

Figure 3: Mean error for position, velocity and attitude, for differing sampling rates.

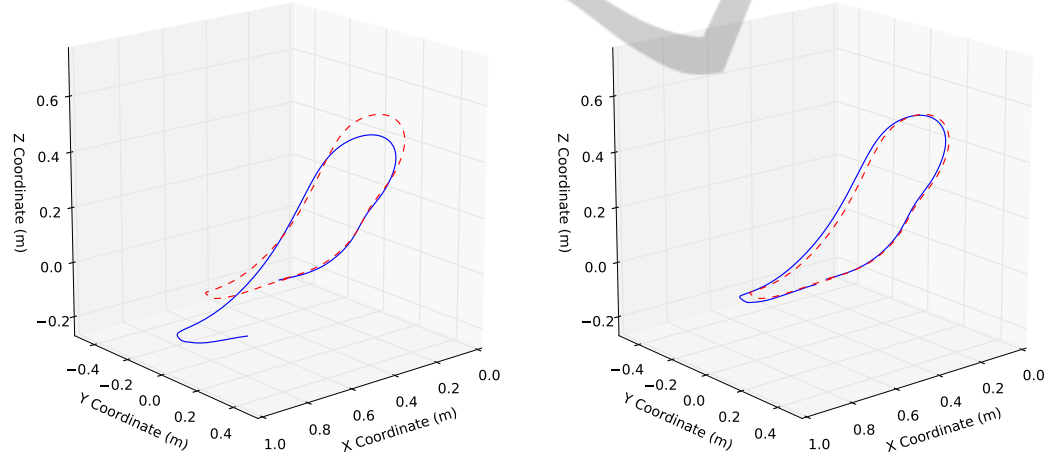

(a) 125Hz (b) 250Hz

Figure 4: Figures showing a single step's trajectory recovery at two different sampling rates.

for 3 participants (2 male, 1 female) and 5 surfaces. The 5 surfaces tested were picked as likely scenarios for outdoor running. Surfaces chosen were running track, astro turf, tarmac, gravel, and grass.

Participants were asked to run on each of the different surfaces, which were located in the same area. Each participant ran 100 meters on each surface. The data were then segmented into steps, midstance-midstance and from each step the peak acceleration was recorded.

Participants were asked to run at a self-selected speed that would be representative of their steady state running. The speed of each participant's run was estimated using a linear dedrifted strapdown algorithm (Bailey and Harle, 2014; Mariani et al., 2010). This was chosen over a Kalman filter based approach due to the lower number of steps logged. The linear dedrift method does not need time for a filter to settle and so was better suited to these shorter runs with similar levels of accuracy as verified by previous stud-

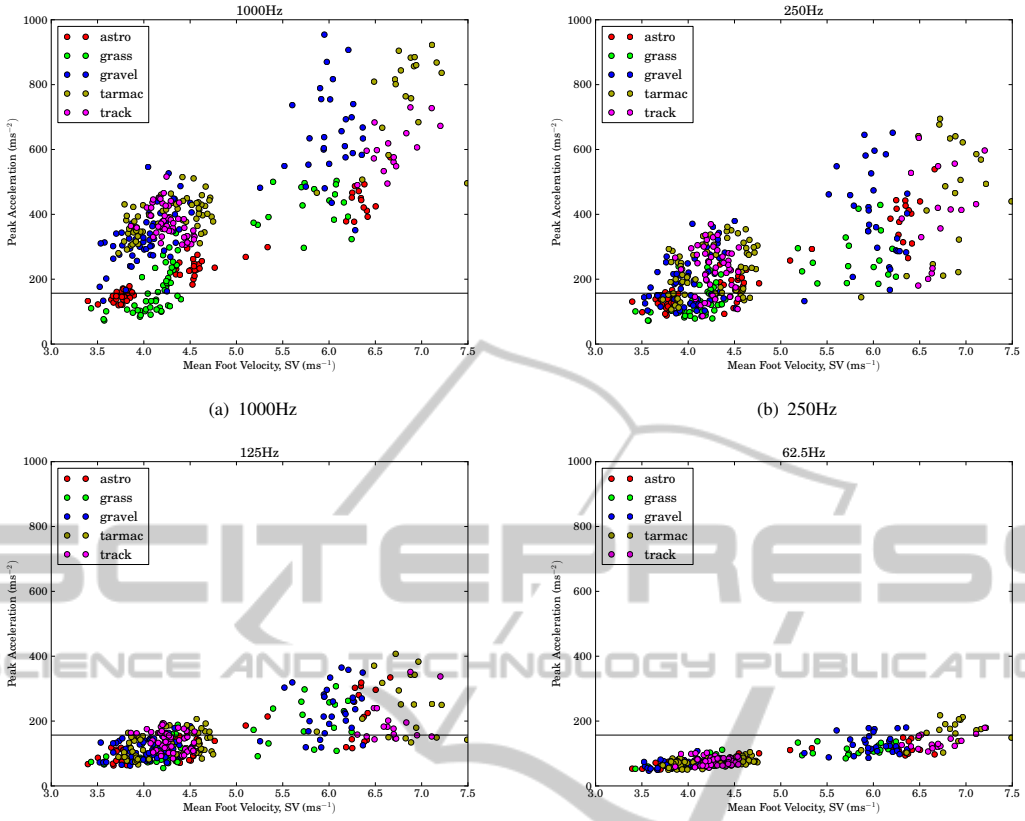

(a) 1000Hz (b) 250Hz

(c) 125Hz (d) 62.5Hz

Figure 5: Figures showing peak acceleration plotted against mean foot speed for each step. The horizontal lines marks the limit of the 16g sensor above which the sensor with a $\pm$16g range would saturate.

ies.

The results obtained show that the largest factor in peak acceleration was the foot speed but that surface also affected requirements. Figure 5 shows the impact acceleration for all steps logged plotted against the mean foot velocity (SV) for each step. SV was defined as in (Mariani et al., 2010), that is mean velocity in the ground plane (the XY plane). For each step, between midstance events, the following was calculated:

$$SV(i) = \frac{\sum_{k=0}^{N_i} \sqrt{v_x(i,k)^2 + v_y(i,k)^2}}{N_i} \quad (4)$$

where i is the step number, k is the sample number within step i, and N_i is the number of samples within step i.

Figure 5 shows that even at 62.5Hz there were a few samples that would saturate a 16g sensor at higher speeds. At 1kHz the majority of steps would show sensor saturation with a 16g sensor and the situation improves only slightly at 250Hz, the point which we found to be the optimal sampling rate.

Mean and max peak accelerations are shown in Table 1 showing high maximum accelerations on tarmac of around 90g. Study of peak gyroscope signals were inconclusive as at higher speeds the sensor saturated and it was not possible to obtain a higher range sensor than the $\pm$2000°s^{-1} sensor contained in the MPU-6000. Figure 6 shows the data obtained at the 1kHz sampling rate, sensor saturation can be seen at higher speeds.

4.3 Effect of Saturation on Measurement Accuracy

While sensor saturation has been suggested as a potential factor that may decrease accuracy of measurement results no work has yet investigated how significant the loss in accuracy might be. Here we compare the accuracy of results using the 16g accelerometer only, to that which replaces saturated samples with those taken from the 200g accelerometer.

This investigation re-uses the data listed in section 4.1 and the Extended Kalman Filter was applied in

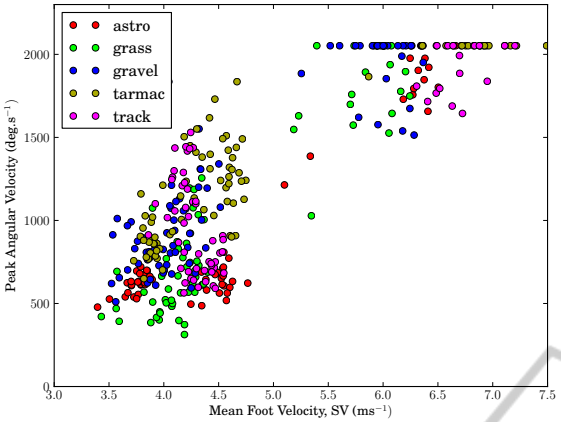

Figure 6: Plot of maximum rate against mean foot speed showing saturation of the $\pm 2000^{\circ}s^{-1}$ gyroscope.

Table 1: Mean and maximum step accelerations for the accelerometer.

Sampling Rate (Hz)	Surface	Mean (ms^{-2})	Max. (ms^{-2})
1000	astro	244	575
	grass	229	503
	gravel	438	954
	tarmac	481	922
	track	430	729
250	astro	207	539
	grass	168	428
	gravel	261	651
	tarmac	286	694
	track	272	635

the same manner. However the filter was run twice, once with the data as described in section 3.3 and once with data from only the 16g accelerometer containing sensor saturation. The data were processed for the highest sampling rate available, 1kHz.

Error statistics were calculated as in 4.1 to give error values for each sample in each step. Subsequently, for each step, the maximum and mean errors were calculated for position, velocity and attitude. For example $s^{error}_{max}(i) = max_k(s^{error}(i,k))$ and $s^{error}_{mean}(i) = mean_k(s^{error}(i,k))$ give the maximum error in position and the mean error in position for step i. These statistics were similarly calculated for velocity and attitude. The mean and standard deviation for these statistics are presented in Table 2.

The results show an increase in the error for the 16g only trajectory recovery. Table 2 shows the results for the fastest treadmill speed recorded, $3.4ms^{-1}$. It can be seen that there is a reduction in the mean and maximal error when using the combined 16g/200g sensor as opposed to 16g only.

As an example of a potentially interesting metric that could be calculated, the mean foot velocity was also assessed over all steps. Mean foot velocity (SV) was calculated as defined in section 4.2.

Bias, standard deviation and limits of agreement were calculated for the SV metric over all steps for both sensor setups. Using the combined setup the bias and standard deviation were $0.007 \pm 0.0156ms^{-1}$ with limits of agreement $-0.023ms^{-1}$ to $0.038ms^{-1}$. Using the 16g only sensor the bias and standard deviation were $0.006 \pm 0.020ms^{-1}$ with limits of agreement -$0.033ms^{-1}$ to $0.044ms^{-1}$. Bland-Altman plots for the results can be seen in Figure 7. Both show some correlation in error with speed and the combined sensor setup shows slightly tighter limits of agreement. However, both sensor setups produce a level of accuracy that may be useful for this metric.

Table 2: Mean and standard deviation of per-step metrics for different sensor setups at 1kHz while running at $3.4ms^{-1}$.

Measurement	Sensor	Mean and SD
s^{error}_{max}(m)	Combined	0.087 ± 0.061
	16g	0.142 ± 0.115
s^{error}_{mean}(m)	Combined	0.048 ± 0.033
	16g	0.079 ± 0.063
$v^{error}_{max}(ms^{-1})$	Combined	0.52 ± 0.12
	16g	0.60 ± 0.21
$v^{error}_{mean}(ms^{-1})$	Combined	0.16 ± 0.08
	16g	0.24 ± 0.15
θ^{error}_{max}(Deg)	Combined	3.30 ± 0.90
	16g	4.71 ± 1.85
θ^{error}_{mean}(Deg)	Combined	1.77 ± 0.71
	16g	2.98 ± 1.48

5 CONCLUSIONS

This work has shown that a trade off in sampling rate is possible in order to obtain lower sensor requirements. Extended Kalman Filter based trajectory recovery seems to be little affected by sampling rates until below 250Hz. However at 250Hz there would still be regular saturation in overground running on outdoor surfaces using a $\pm 16g$ accelerometer.

We also show that sensor saturation does affect the accuracy of the trajectory recovery. We found that the addition of a high range accelerometer resulted in up to a 40% reduction in error for some metrics, for example the reduction of mean attitude error reduced from 2.89° to 1.77°. However, it remains unclear how much larger peak accelerations present in higher speeds in an outdoor scenario would affect the accuracy as we were limited in the maximum speed of the treadmill. As such, it remains unclear as to how the

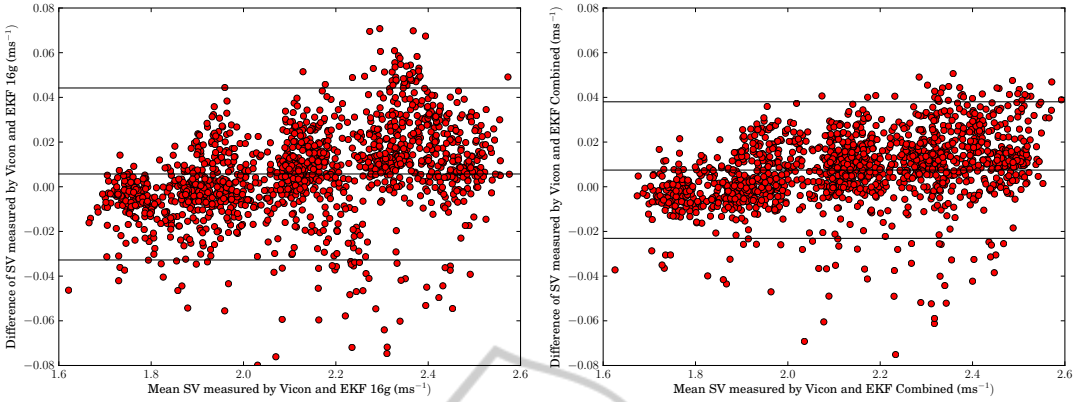

(a) 16g (b) Combined

Figure 7: Bland-Altman plots for SV as calculated from Combined and 16g sensor data.

method would perform for elite endurance athletes at greater running speeds. Further research should seek to attempt to evaluate these methods at higher speed.

We have been unable to assess requirements for the range in angular velocity measurement to inform gyroscope selection due to limitations in our sensor at higher speeds and it may prove difficult to test in the future due to the lack of commercial availability of MEMS gyroscopes that have a higher range than the $\pm 2000^{\circ}s^{-1}$ one used in this paper. Further work may therefore seek to assess whether or not gyroscope saturation has a significant affect on measurement accuracy. If it is found to affect results further work should seek to mitigate these periods of saturation if possible.

REFERENCES

Bailey, G. and Harle, R. (2014). Assessment of Foot Kinematics During Steady State Running Using a Foot-mounted IMU. *Procedia Engineering*, 72:32–37.

Bichler, S., Ogris, G., Kremser, V., Schwab, F., Knott, S., and Baca, A. (2012). Towards high-precision IMU/GPS-based stride-parameter determination in an outdoor runners' scenario. In *Procedia Engineering*, volume 34, pages 592–597.

Foxlin, E. (2005). Pedestrian tracking with shoe-mounted inertial sensors. *IEEE Computer Graphics and Applications*, 25(6):38–46.

Harle, R., Taherian, S., Pias, M., Coulouris, G., Hopper, A., Cameron, J., Lasenby, J., Kuntze, G., Bezodis, I., Irwin, G., and Kerwin, D. G. (2011). Towards real-time profiling of sprints using wearable pressure sensors. *Computer Communications*.

Mariani, B., Hoskovec, C., Rochat, S., Büla, C., Penders, J., and Aminian, K. (2010). 3D gait assessment in young and elderly subjects using foot-worn inertial sensors. *Journal of Biomechanics*, 43:2999–3006.

Mizrahi, J. (2000). Effect of fatigue on leg kinematics and impact acceleration in long distance running. *Human Movement Science*, 19(2):139–151.

Munoz Diaz, E., Heirich, O., Khider, M., and Robertson, P. (2013). Optimal sampling frequency and bias error modeling for foot-mounted IMUs. In *International Conference on Indoor Positioning and Indoor Navigation*, pages 1–9. IEEE.

Peruzzi, A., Della Croce, U., and Cereatti, A. (2011). Estimation of stride length in level walking using an inertial measurement unit attached to the foot: A validation of the zero velocity assumption during stance. *Journal of Biomechanics*, 44:1991–1994.